Title

A New Gridding Method for Zonal Travel Activity and Emissions Using Bicubic Spline Interpolation

Authors

Zheng, Yi
Wang, Bo
Zhang, H. Michael
et al.

Publication Date

2003-09-01

A New Gridding Method for Zonal Travel Activity and Emissions Using Bicubic Spline Interpolation

Yi Zheng, Bo Wang, H. Michael Zhang, Debbie Niemeier*

University of California, Davis

Abstract. For air quality dispersion models, mobile source emissions, including both link- and traffic zone-level emissions, must be disaggregated into grid cells. Current gridding methods assign all traffic analysis zone level emissions to the single grid cell containing the TAZ centroid. In this study, we propose a new approach for disaggregating traffic analysis zone-level emissions using a bicubic spline interpolation function and activity and roadway densities. The new approach, which betters replicates the heterogeneity associated with travel activities, distributes zone-level emissions into the grid cells contained within the zone boundary. When results are compared to the current methods, we find that fewer grid cell misallocations occur and that emissions from TAZs overlapping multiple grid cells are apportioned correctly. The gridded emission inventory developed using the new approach will result in better data inputs for air quality modeling, and in particular can significantly improve transportation conformity analysis.

Keywords: Bicubic Spline Interpolation, Spatial Allocation, Disaggregation, Gridded, Zone-level, Mobile Source Emission.

Corresponding Author:
Debbie Niemeier, Ph.D., P.E.
Department of Civil and Environmental Engineering
One Shields Ave.
University of California
Davis, CA 95616
(530) 752-8918
(530) 752-7872 (Fax)
dniemeier@ucdavis.edu

A New Gridding Method for Zonal Travel Activity and Emissions Using Bicubic Spline Interpolation

Yi Zheng, Bo Wang, H. Michael Zhang, Debbie A. Niemeier
University of California, Davis

INTRODUCTION

Both transportation conformity and photochemical air quality modeling rely on gridded mobile source inventories for analysis. Mobile source inventories are a summation of three categories of emissions: interzonal running emissions, interzonal start and park emissions, and intrazonal emissions. Interzonal running emissions are running hot stabilized emissions resulting from travel between traffic analysis zones (TAZs). Interzonal start and park emissions result from a vehicle's interzonal engine-on (starts) and park events occurring at each end of an interzonal trip, and finally, intrazonal emissions include all intrazonal running hot stabilized and intrazonal start and park (or trip end) emissions encompassed within a single TAZ.

Interzonal running emissions are currently estimated at the link-level while interzonal starts/parks and intrazonal emissions are currently estimated at the traffic analysis zone (TAZ) level. Most of the currently available gridded mobile source emission inventory models, such as IMPACT (Dresser, 1991), DTIM (SAI, 2001), and even the recent GIS applications (e.g., Brandmeyer *et al.* 2000, Kinnee *et al.* 2001, Possiel *et al.* 2001, Mandya, *et al.* 2002) focus only on disaggregating link-level emissions into grid cells. This is partially because the disaggregation is relatively straightforward and because the interzonal running events have, at least to date, been the major emission-producing event. TAZ-level emissions are usually just assigned to the grid cell in which the TAZ centroid is located. This simplified zonal emission allocation method of placing total TAZ emissions into the centroid grid cell carries with it two limitations.

First, air quality dispersion models are now typically using grid cell resolutions between 1 and 5 km (e.g., Harley *et al.* 1993, Kumar *et al.* 1994, Salvador *et al.* 1999, and Mendoza-Dominguez *et al.* 2000). Thus, depending on the size of the TAZs, there may be any number

of grid cells contained within a single TAZ boundary. As the resolution of photochemical models has increased, in part to better estimate secondary formation of pollutants, the allocation of multiple grid cells' emissions to a single grid cell is increasingly problematic.

The second limitation arises because as stricter tailpipe standards have been implemented, running exhaust emissions account for an increasingly smaller percentage of the total mobile source emissions and intrazonal and interzonal trip-end start and park emissions for an increasingly greater percentage. In some cases, TAZ-level emissions can contribute up to half of the total vehicle emissions in a modeling network (e.g., 48.7% of morning peak 2005 emissions for Sacramento Area of Councils of Governments SACMET network).

To allocate non-mobiles source emissions fractions of surrogate indicators, such as housing, population, and land use are often used to calculate gridded spatial allocation factors (e.g., Sellars *et al.* 1985) These factors are then used to apportion estimated area-wide emissions to individual grid cells. For example, Funk *et al.* (2001) used GIS to develop spatial allocation factors on area source emissions for the modeling domain of California Regional Particulate Air Quality Study and the Central California Ozone Study. Surrogate data on demographics, socio-economics, land use, land cover, and area source facility locations were obtained from various sources. Non-mobile area source emissions were then disaggregated to grid cells based on the fraction of surrogates contained within the grid cell.

This concept of spatially allocating emissions by proxy variables has also been applied in estimating the gridded TAZ-level mobile emissions in a few more recent mobile-source emission models. The EMS-95 model (LADCO, 1998) developed spatial allocation factors for TAZ-level mobile emissions by overlaying a landuse/census ARC/INFO® coverage and a transportation modeling grid ARC/INFO® coverage. In the SMOKE model (MCNC, 2002) county-based mobile emissions are apportioned to grid cells based on the fraction of the area from each county that intersects with the grid cells overlapping that county, or as a fraction of surrogates (e.g., population and length of major freeway).

All of these methods are based on a simple assumption: the distribution of emissions approximates that of the area fractions of selected surrogate indicators in the grid cells. This fraction-based allocation methodology results in a uniformly distributed emission density across the grid cell area (e.g., amount of emissions per km^2), which is generally not applicable for mobile source emissions. For example, we expect mobile source running emissions to be continuous along roadways and start/park emissions, associated with productions and attractions, to be generally concentrated and decrease with distance from the concentrated areas. For these emissions, whose density changes continuously, the fraction-based method cannot replicate the heterogeneous nature of the mobile source emissions.

In this paper, we present a new bicubic spline interpolation approach for allocating TAZ-level mobile source emissions into grid cells. We begin by presenting a new gridding algorithm and then conduct an evaluation study by comparing the new gridding results to the results generated by method most commonly used in California.

PROPOSED METHODOLOGY

To disaggregate TAZ-level vehicle emissions into grid cells, we propose a disaggregation methodology based on non-uniform continuous functions. In the gridded network, the modeling domain region is composed of equally sized grid cells. Denoting E^l as the total TAZ-level emissions in the modeling domain by pollutant type l =1, 2, 3, 4 (e.g., total organic gases, carbon monoxide, nitrogen oxide, and carbon dioxide), and denoting E_i^l as the portion of TAZ level emissions contained within grid cell i. The sum of grid cell emissions E_i^l should be equal to the total emissions of the modeling domain E^l (Equation 2),

$$E^l = \sum_{i=1}^{\gamma} E_i^l \tag{2}$$

where γ is the number of grid cells in the entire modeling region. For grid cell i, we can also denote f_i^l as the spatial allocation factor used to disaggregate total emissions E^l into grid cell i. Therefore, E_i^l for any given grid cell i can be expressed as,

$$E_i^l = E^l \cdot f_i^l \tag{3}$$

where $\sum_{i=1}^{\gamma} f_i^l = 1$. The question then becomes one of estimating f_i^l. Since we use the same methodology to develop allocation factors for each type of pollutant, the pollutant index l is dropped for simplicity.

It is reasonable to assume that allocation factor f_i is a function of both activities (interzonal trip-end activities are the sum of interzonal productions and attractions reported by a travel demand model; intrazonal activities are the intrazonal trip volumes reported by a travel demand model) that occur within grid cell i and the roadway density of grid cell i (Equation 4),

$$f_i = f \text{ (activities, roadway density)} \quad (4)$$

While roadway densities can be computed directly for any given grid cell using the information from the transportation network, activities information resides at the TAZ level. To develop allocation factors for each grid cell, we begin by disaggregating the TAZ-level activity information into grid cells.

As discussed in the literature review section, the GIS-based methods process the disaggregation using an evenly distributed density function (e.g., assuming number of activities per km^2 unchanged across the cell area), which is obviously not true in the real world. Given the nature of mobile emissions, we expect the spatial distribution of activity density (number of activities per km^2) to be a non-uniform continuous function.

Consider that we have two TAZs producing and attracting approximately the same number of trips, but having different areas. Since, by definition, grid cells are equal in size for air quality modeling, the number of grid cells contained within the smaller TAZ will be less than the number within the larger TAZ. Thus, each grid cell of the smaller TAZ should have proportionally more travel activities than the grid cells contained within the larger TAZ. Therefore, activity density can be used to distinguish TAZs from each other at the grid cell level. In travel demand modeling, TAZs typically encompass generally homogeneous travel activities and the TAZ centroid, usually located at the point of the greatest activity density, is

labeled to represent the activities of that TAZ. This allows us to reasonably assume that the activity density of the grid cell in which the TAZ centroid is located is approximately equal to the activity density of the TAZ. We can use a bicubic spline interpolation approach to disaggregate TAZ activities to grid cells based on activity density, which can link zone and grid cell during the interpolation procedure.

To disaggregate the emissions, we first calculate TAZ activity densities at each centroid. Then we use bicubic spline interpolation to estimate activity densities for all grid cells in the modeling region, which can give us the grid cell-level number of activities when multiplying by the grid cell size. This interpolation-based disaggregation method computes gridded activities based on a non-uniform continuous density function and thus more closely replicates the heterogeneous nature of mobile activities.

The proposed methodology can be described in the following four steps,

Step 1: Calculation of TAZ activity density at each TAZ centroid;
Step 2: Transformation of TAZ activity densities to mesh points;
Step 3: Computation of grid cell level activity densities, and
Step 4: Computation of allocation factors.

Calculation of Trip Density at Each TAZ Centroid

We begin by creating a $(m+1)\times(n+1)$ mesh that encompasses the entire modeling region, where m and n are user-defined values that reflect the numbers of equal-distance mesh points in the horizontal, x, and the vertical, y, directions. In a travel demand model, the TAZ-level intrazonal activities are reported as a single value for each TAZ and interzonal trip-end activities are reported separately as interzonal productions and attractions for each TAZ. Because all activities are reported at each TAZ centroid, TAZ intrazonal activity density or interzonal trip-end activity density (d_j) can be calculated at TAZ j's centroid by dividing the TAZ intrazonal activities or interzonal trip-end activities (t_j) by the TAZ area (A_j). Note that the TAZ interzonal trip-end activities are the sum of interzonal productions and attractions.

$$d_j = \frac{t_j}{A_j} \tag{5}$$

Transformation of TAZ Activity Densities to Mesh Points

The commonly used bicubic spline interpolation methods require that input data be located uniformly at the intersections (mesh points) of the x-direction and y-direction grid lines in the modeling domain (Shikin *et al.* 1995). However, the travel demand modeling TAZ centroids are usually scattered throughout the domain. Therefore, to perform the activity density interpolation, we have to transform activity density from the scattered centroid points to the uniform mesh points.

Since our activity density distribution is continuous, densities at each mesh point are correlated to each other. Using the inverse of the distances between a TAZ centroid and mesh points, we can distribute activity densities from scattered TAZ points into the uniform mesh points,

$$z_{cd} = \sum_{j=1}^{\delta} \frac{d_j}{\sqrt{(x_c - x_j)^2 + (y_d - y_j)^2}} \tag{6}$$

where

z_{cd} = Transformed activity density at mesh point (x_c, y_d)

x_c, y_d = x and y coordinates of mesh point $(c = 0,1,...,m)$ and $(d = 0,1,...,n)$

x_j, y_j = x and y coordinates of TAZ j's centroid $(j = 0,1,...,\delta)$

This function is conceptually similar to that of impedance functions where the mesh points furthest from the TAZ centroid are assigned a lower proportion of the activity density from that TAZ. After all centroid activity densities are distributed to the $(m+1)\times(n+1)$ mesh points, the transformed densities, z_{cd}, and the associated mesh point coordinates, x_c $(c = 0,1,...,m)$ and y_d $(c = 0,1,...,m)$, are available for interpolation.

Computation of Grid Cell Activity Densities

We use a bicubic spline interpolation (e.g., Shikin *et al.* 1995) to disaggregate activity densities, which are intrazonal trip or interzonal trip-end densities, into grid cells. In the mesh, we define a rectangle area $R=[a,b]\times[g,h]=\{(x,y)\,|\,a\le x\le b,\ g\le y\le h\}$ with a mesh point ω is defined as $\omega=\omega_x\times\omega_y$ where $\omega_x: a=x_0<x_1<...<x_{m-1}<x_m=b$ and $\omega_y: g=y_0<y_1<...<y_{n-1}<y_n=h$. At mesh point ω, we know the activity density z_{cd}, $(c=0,1,...,m,\ d=0,1,...,n)$, from which a bicubic spline interpolation function can be defined as

$$S(x,y)=\sum_{p=0}^{3}\sum_{q=0}^{3}a_{p,q}^{(c,d)}(x-x_i)^p(y-y_j)^q \qquad (x,y)\in R. \tag{7}$$

which satisfies two conditions: (1) $S(x,y)$ and its derivatives $\frac{\partial S}{\partial x}$, $\frac{\partial S}{\partial y}$, $\frac{\partial^2 S}{\partial x^2}$, $\frac{\partial^2 S}{\partial y^2}$, $\frac{\partial^2 S}{\partial x\partial y}$, $\frac{\partial^3 S}{\partial x^2\partial y}$, $\frac{\partial^3 S}{\partial x\partial y^2}$, $\frac{\partial^4 S}{\partial x^2\partial y^2}$ are continuous in R, and (2) $S(x_c,y_d)=z_{cd}$. The boundary conditions are defined as: (1) the values of the second partial derivatives of the function $S(x_c,y_d)$ with respect to x and y are given at the boundary knots of ω, $\frac{\partial^2 S}{\partial x^2}(x_c,y_d)=z_{cd}$, $\frac{\partial^2 S}{\partial y^2}(x_c,y_d)=z_{cd}$, and (2) the values of the mixed fourth derivative $\frac{\partial^4 S}{\partial x^2\partial y^2}$ are given at the four corner knots of ω, $\frac{\partial^4 S}{\partial x^2\partial y^2}(x_c,y_d)=z_{cd}$.

Therefore, for any given grid cell i, the unknown activity density, d_i, can be computed by $d_i=S(x'_i,y'_i)$, where x'_i and y'_i are central point coordinates of grid cell i. The grid cell i's activities, t_i, thus, can be obtained by multiplying the grid cell activity density by the grid cell size, $t_i=d_i\times a_i$, where a_i is the area of grid cell i.

Computation of Allocation Factors

In this step, the activities for each grid cell are combined with grid cell facility-specific roadway density (roadway link length divided by the area of grid cell) to compute allocation factors.

Using the grid cell level activities, t_i, the weighting factor for grid cell i is defined as,

$$F_i = t_i \cdot (FW_i \cdot R_\lambda + RL_i \cdot R_\varphi), \quad (8)$$

where the freeway roadway density, FW_i, is defined by dividing the length (km) of freeways contained within grid cell i by the grid cell area (km^2), the roadway density of arterial and other facilities, RL_i represents the roadway density for arterials and other types of facilities contained within grid cell i, and R_λ and R_φ denote the emission factors for freeways and arterials and other facilities, respectively.

Note that the right hand side of Equation 8 comprises two parts. The first part, t_i, represents the grid cell trips. When calculating the allocation factors for intrazonal emissions (intrazonal running, start and park emissions), t_i is taken to be the grid cell level intrazonal trip volume. When calculating the allocation factors for interzonal trip-end emissions (interzonal start and park emissions), t_i is taken to be the grid cell level interzonal trip-ends (e.g., productions and attractions). In the latter part of Equation 8, $FW_i \cdot R_\lambda + RL_i \cdot R_\varphi$ reflects the emission contribution of roadways. Obviously, higher roadway densities not only lead to higher running emissions, but can also induce increased start and park emissions. FW_i and RL_i also restricts the allocation of TAZ-level emissions to only those grid cells that contain roadways because the weighting factor, F_i, for a grid cell will become zero when FW_i and RL_i approach zero. Also, since traffic conditions (e.g., vehicle speed and traffic volume) vary by facility and produce different effects on emissions, R_λ and R_φ are intended to replicate the contributions of facility types to the emissions allocation. We can use emission factors to represent facility contribution factors. Finally, the spatial allocation factor f_i for each grid cell i can be computed by

$$f_i = \frac{F_i}{\sum_{i=1}^{\gamma} F_i} \tag{9}$$

EVALUATION OF THE METHODS

To test the new gridding algorithm we use the Sacramento Area Council of Governments (SACOG)'s SACMET network (Figure 1), comprising 11272 nodes, 1139 TAZs, and 18624 links. The transportation data obtained from SACOG include a MINUTP road network for the SACMET travel demand model, TAZ areas (km^2), and year 2000 weekday morning-peak intrazonal volumes and weekday morning-peak interzonal productions and attractions. The SACMET network provides information on link facility types and node coordinates for both link nodes and TAZ centroids. Five urban areas (Woodland, Davis, Sacramento, Placerville, and Auburn) can be identified in the network.

[insert Figure 1]

We used the common airshed model grid cell size of 4×4 km. The roadway length by facility types in each grid cell is calculated by searching for the intersection of links and grid cell boundaries. The algorithm begins by reading a link record from the SACMET network. Using Equation 10, the link's begin node is assigned to a grid cell, identified by the grid cell indexes in the x and y directions.

$$\begin{aligned} index\_x &= Integer[(x\_coordinate - x\_org) \div \Delta x] \\ index\_y &= Integer[(y\_coordinate - y\_org) \div \Delta y] \end{aligned} \tag{10}$$

where

$index\_x$, $index\_y$ = Grid cell's index in the x and y directions in the domain

$x\_coordinate$, $y\_coordinate$ = Link node's x and y coordinates

x_org, y_org = x and y coordinates of the bottom-left corner in the domain

$\Delta x, \Delta y$ = Grid cell width in x and y directions

Next, we calculate the slope of the link based on the coordinates of the link's begin/end nodes; the slope of the first dashed line in Figure 2 is calculated using the coordinates of the begin node and the upper-right corner of the grid cell. The algorithm then finds the first

intersection of the link and grid cell boundary by comparing these two slopes. In Figure 2, when the link slope is less than the first dashed line slope, the x coordinate of the first intersection (point "A") should equal to the grid cell boundary's x coordinate "X_1", and the y coordinate of "A" can be calculated by "X_1"and link slope. When the coordinates of the begin node and "A" are known, the portion of the link falling within the first grid cell can be calculated. This portion of the link is then accumulated into the grid cell identified by the grid cell indexes.

[insert Figure 2]

Node "A" then becomes the next begin node of the link. Equation 10 is again applied to allocate "A" to another grid cell. In searching for the next intersection, "B", in Figure 2, since the link slope is higher than the second dashed line slope, the grid cell boundary's y coordinate "Y_1" becomes the y coordinate of "B", and the x coordinate of "B" is calculated using "Y_1" and the link slope. The portion of the link distance falling within the second grid cell is calculated and the distance is accumulated. This computation is continued to the end of link. After all the link records are processed, the link length by facility type will have been computed for each grid cell.

To compute the activity density for each TAZ, intrazonal activities and interzonal trip-ends (productions/attractions) are divided by the respective TAZ areas. This information, grid cell-based link length by facility types, TAZ intrazonal activity density, and interzonal trip-end density, can be used to develop spatial allocation factors. Default R_λ and R_φ values in Equation 8 are taken from California Air Resources Board's MVEI7G trip-based emission factor model. We assume an average intrazonal freeway running speed of 65 mph and an arterials/others speed of 30 mph, which are common California's speed limits for these facilities. Users can update the default R_λ and R_φ using local emission factor inputs.

[insert Table 1]

RESULTS

We conducted a comparison of the new method to the most commonly used method in California, which is to assign the complete TAZ-level emissions into the grid cell that contains the TAZ centroid. DTIM4, (version: Dec. 2001), which is the approved mobile

source emission inventory model for California, uses this method for allocating TAZ emissions to grid cells. We compared the new morning peak modeling results to those generated using the DTIM4 centroid approach, holding all others variables constant.

Gridded Intrazonal Emissions

The SACOG travel demand model reports the intrazonal (running stabilized) trips and intrazonal trip-ends (starts and parks). These activities generate TAZ-level intrazonal emissions, including intrazonal running, start, and park emissions that must be accounted for in a vehicle emissions inventory model. Figure 3 shows the spatial distribution of TAZ centroids across the SACMET modeling region and the associated TAZ intrazonal activity densities from different perspectives As might be expected, the spatial distribution of activity densities is heterogeneous with higher densities in downtown Sacramento and continuously decreased densities in the surrounding areas. The maximum intrazonal activity densities occur in downtown Sacramento area (90 km $\leq$ x $\leq$ 105 km and 50 km $\leq$ y $\leq$ 65 km). TAZs in rural areas are usually very large and thus should have lower intrazonal activity densities. This is also seen in Figure 3, where the TAZs located near the network border (y $\leq$ 20 km or y $\geq$ 130 km in Figure 3b; x $\leq$ 28 km or x $\geq$ 180 km in Figure 3c) carry the lowest intrazonal activity densities.

[insert Figure 3]

Figures 4 shows the grid cell level intrazonal activity densities after the interpolation, which ranges from 0 to 72 activity/km^2. The TAZ activity densities ranged from 0 to 1400 activity/km^2, the lower activity densities at the grid cell level are due to the average of high activity densities and low activity densities in a large grid cell. For example, a TAZ in downtown Sacramento can be as small as 25 acres (0.101 km^2) in size with a high activity density, which is overlaid with a grid cell resolution of 4×4 km (16 km^2) that will encompass some adjacent TAZs with relatively lower activity densities. Considering the mixture of high and low activity density TAZs in some grid cells, the range of grid cell activity densities in Figure 4 is expected.

[insert Figure 4]

We also calculated the total number of grid cell level intrazonal activities in Figure 4 as 106,115 for the region. This compares to the original sum of TAZ intrazonal trips of 104,553. That is, the interpolated grid cell level trips are 1.5% higher; most of the extra activities occur around the network border (e.g., the area of $x \leq 20$ km and 48 km $\leq y \leq 92$ km). The extra activities are due to the nature of bicubic spline interpolation, which has no control on curve fittingoutside the interpolation region. In our model, these extra activities will have negligible effect on the computation of allocation factors using Equation 8, because the grid cell roadway densities in these areas are zero.

Applying the calculated allocation factors to TAZ AM-peak intrazonal emissions results in the gridded AM-peak intrazonal emissions shown in Figure 5. For comparison, we also show the gridded AM-peak intrazonal emissions using the standard centroid placement method in Figure 6. It is clear from the figures that assigning total TAZ emissions to the grid cell containing the centroid results in a more discrete spatial allocation relative to the bicubic spline method.

Theoretically, grid cell level emissions should be proportional to activity density. That is to say, all things equal,downtown Sacramento, representing the highest activity density in the modeling domain, should also produce the highest gridded emissions (Figure 5). Since the standard method apportions the entire TAZ emissions to the centroid grid cell, then the larger the zone the more likely it is that an unrealistic spike in the emissions will also be produced. In Figure 6, the maximum gridded intrazonal emissions are not located in the Sacramento downtown area where we might expect, but instead in a very large, predominantly rural TAZ centroid grid cell identified on the figure as “TAZ Max”.

In Figure 5, it becomes apparent that most of the emissions in this TAZ are likely associated with a freeway transecting the TAZ. In the case of a large TAZ, this type allocation error can occur often in a gridded emission inventory using the centroid approach.

[insert Figure 5 and Figure 6]

Figure 6 can also be used to examine the accuracy of the proposed gridding methodology. The gridded emissions in a grid cell usually comprise two parts: emissions from the TAZs that are completely contained within a particular grid cell boundary and the portion of TAZ emissions that fall only partially within the grid cell boundary (e.g., emissions spanning more than one grid cell). In downtown Sacramento, where a larger resolution grid cell can encompass more than one downtown TAZ, because TAZs are much smaller in area than the specified 4x4 km grid resolution, the standard method, which assigns TAZ emissions completely into the centroid grid cell, successfully allocates emissions from TAZs that fully encompassed by the grid cell. Thus, we would expect that the gridded emissions in downtown Sacramento computed using the new methodology should be equal to or higher than the downtown gridded emissions produced using the standard method.

As can be seen, the maximum gridded emission in Figure 5 is 15 kg in the downtown Sacramento area, which is very close to the peak gridded emissions (14 kg) using the standard method (Figure 6). This indicates that 1 kg of emissions comes from emissions produced by TAZs that are only partially contained within the grid cell boundary.

Gridded Interzonal Trip-End Emissions

Interzonal trip-end travel activities include interzonal starts and parks, whose emissions are computed at the TAZ level and do not include interzonal running activities whose emissions are computed at the link level. Figure 7 shows the interzonal TAZ trip-end activity density from different perspectives.

Figure 8 shows the grid cell level interzonal trip-end activity density after the bicubic spline interpolation. The figure suggests a greater number of interzonal trip-ends originated and destined for downtown areas; as might be expected, this pattern is less significant for intrazonal activities. We can see that the highest interzonal trip-end activity densities are located in downtown Sacramento, which is consistent with the spatial distribution in Figure 7. The sum of the grid cell interzonal trip-end activities calculated from Figure 8 is 2,325,727 for the network, which compared to the sum of TAZ interzonal productions and attractions, 2,282,350, is within 1.9%.

[insert Figures 7 and 8]

The gridded AM-peak interzonal trip-end emissions using both the new and standard methods are shown in Figures 9 and 10. When comparing the proposed method to the standard method, we again tend to find a more discrete pattern of allocation using the standard method (Figure 9). We also can also see the same problem of incorrectly assigned peaks in emissions (TAZ Max1, TAZ Maz2).

We computed the maximum grid cell emissions in Figure 9 at 120 kg in downtown Sacramento, while Figure 10 resulted in a downtown Sacramento grid cell emission of 103 kg. This suggests that allocating the emissions using the standard approach can result in a fairly difference. For example, in the downtown Sacramento case just discussed, the difference between the emissions estimates results from partial TAZ allocations that are not considered in the standard method.

[insert Figures 9 and 10]

CONCLUSION AND DISCUSSION

In this study, we focused on the spatial disaggregation of intrazonal emissions and interzonal trip-end emissions, which use TAZ level activities produced by travel demand forecasting. We tested a new bicubic spline interpolation method for apportioning emissions using the Sacramento Area Council of Governments (SACOG)'s SACMET network. These gridded emissions were then compared to gridded emissions produced using the standard protocol of assigning TAZ emissions are to the centroid cells. The comparison study shows that the new method improves the gridded emission inventories by better resolving emissions from large TAZs to grid cells within the TAZ and by handling apportionment of emissions in cases where grid cells only partially transect TAZs. For brevity, we only presented the AM-peak allocation factors for total organic gas. Gridded emissions for other time periods and pollutants (CO, NOx, and CO_2) can also be developed using the same methodology.

We identified two limitations associated with the new methodology. First, based on the model formulation (Equation 8), the allocation factor is zero in a grid cell having no link or

producing/attracting no trips. Thus, the quality of the methodology relies on resolution used to code the transportation network. If arterials, for example, are not coded in detail, the allocation factors will be coarse. Second, instead of applying the interpolation directly to the scattered activity inputs, this model uses a pre-processed mesh point transformation. Further improvement may be gained through direct interpolation on scattered activity inputs.

In conclusion, as running emissions account for smaller portions of total mobile source emissions and grid cell becomes smaller, it becomes increasingly important spatially allocate TAZ-level mobile emissions. Accurately allocating TAZ level emissions will impact subsequent dispersion modeling and improve our ability to conduct high quality conformity analyses.

Acknowledgements

This research was partially funded by the National Science Foundation and the University of California Transportation Center. The views are those of the authors alone.

REFERENCES

Bachman,W.H. , A GIS-Based Modal Model of Automobile Exhaust Emissions, Final Report, EPA Cooperative Agreement CR823020, Prepared for: U.S. Environmental Protection Agency, Office of Research and Development, Washington, DC 20460, 1998

Brandmeyer, J.E. and H.A. Karimi, Improved spatial allocation methodology for on-road mobile emissions, Journal of Air & Waste Management Association, 50, 972-980. 2000

CARB, "Methodology for Estimating Emissions from On-Road Motor Vehicles Volume II: EMFAC7G", California Environmental Protection Agency, Air Resources Board, 1996

Dresser, G.B. and C.E. Bell, IMPACT: Highway Pollutant Emission Model User's Guide, Research Report 947-3, College Station, Texas, Texas Transportation Institute, 1991

Funk, T.H., P.S. Stiefer, and L.R. Chinkin, "Development of Gridded Spatial Allocation Factors for the State of California", Technical Memorandum for CARB, by Sonoma Technology Inc, Petaluma, CA, STI-900201/99542-2092-TM, 2001

Harley,R.A. , A.G. Russell, G.J. MacRae, G.R. Cass, and J. Seinfeld, "Photochemical Modeling of the Southern California Air Quality Study", Environmental Science and Technology, Vol. 27, No. 2, 378-388, (1993)

Kinnee, E. and A. Beidler, "Revised Methodology for the Spatial Allocation of VMT and Mobile Source Emissions Data", paper presented at the 10th International Emission Inventory Conference, "One Atmosphere, One Inventory, Many Challenges", sponsored by EPA, Denver, Co, May, 2001

Kumar, N., A. Russell, T. Tesche, and D. McNally, "Evaluation of Calgrid Using Two Different Ozone Episodes and Comparison to UAM Results", Atmospheric Environment, Vol. 28, No. 17, 2823-2845, (1994)

LADCO, EMS-95 User's Guide, Lake Michigan Air Directors Consortium, last updated August, 1998 http://ladco.org/guide/ems95.html (Accessed on June 2, 2002)

Mandya, R.K., S. Kumar, and K. John, "Using Geographical Information System for Distribution of Pollutant Emissions with An Urban Airshed Model Grid System", paper presented at the Fourth Symposium on the Urban Environment, American Meteorological Society, Norfolk, VA, 20–24 May 2002

MCNC, Sparse Matrix Operator Kernel Emissions (SMOKE) Modeling System On-Line User's Guide, MCNC-North Carolina Supercomputing Center, http://edge.emc.mcnc.org/uihelp/docs/smoke.html (Accessed on June 2, 2002)

Mendoza-Dominguez, A. and A. Russell, "Iterative Inverse Modeling and Direct Sensitivity Analysis of a Photochemical Air Quality Model", Environmental Science and Technology, Vol. 34, No. 23, 4974-4981, (2000)

Possiel, N., G. Stella, R. Ryan, and T. Pace, "Development of an Anthropogenic Emissions Inventory for Annual Nationwide Models-3/CMAQ Simulations of Ozone and Aerosols", paper presented at the 10th International Emission Inventory Conference, "One Atmosphere, One Inventory, Many Challenges", sponsored by EPA, Denver, Co, May, 2001

Salvador, R., J. Calbo, and M.M. Millan, "Horizontal Grid Size Selection and its Influence on Mesoscale Model Simulations", Journal of American Meteorological, Vol. 38: 1311–1329, (1999)

Sellars, F.M., T.E. Fitzgerald, J.M. Lennon, N.M. Monzione, and D.R. Neal, "Project Summary, National Acid Precipitation Assessment Program Emission Inventory Allocation Factors", Air and Energy Engineering Research Laboratory, Environmental Protection Agency of the United States, EPA/600/S7-85/035, 1985

Shikin, E.V. and A.I. Plis, *Handbook on Splines for the User*, Boca Raton, CRC Press, Inc. (1995)

Systems Application International, "DTIM4 User's Guide", ICF Kaiser Consulting Group, Systems Applications International, San Rafael, CA, 2001

Table 1. Facility Contribution Factor[1]

	TOG $(l=1)$	CO $(l=2)$	NOx $(l=3)$	CO_2 $(l=4)$
Freeway	$R_{\lambda}^{1} = 0.58$	$R_{\varphi}^{2} = 11.52$	$R_{\varphi}^{3} = 1.25$	$R_{\varphi}^{4} = 326.96$
Arterial and Others	$R_{\varphi}^{1} = 0.22$	$R_{\varphi}^{2} = 3.72$	$R_{\lambda}^{3} = 0.44$	$R_{\lambda}^{4} = 266.27$

[1] (CARB, 1996) MVEI7G Emission Factor Scenario for year 2000, model years 1966-2000 inclusive, summer time. All data in the table are in unit of gram/mile for light duty autos with catalyst-equipped.

Figure 1. SACMET Network

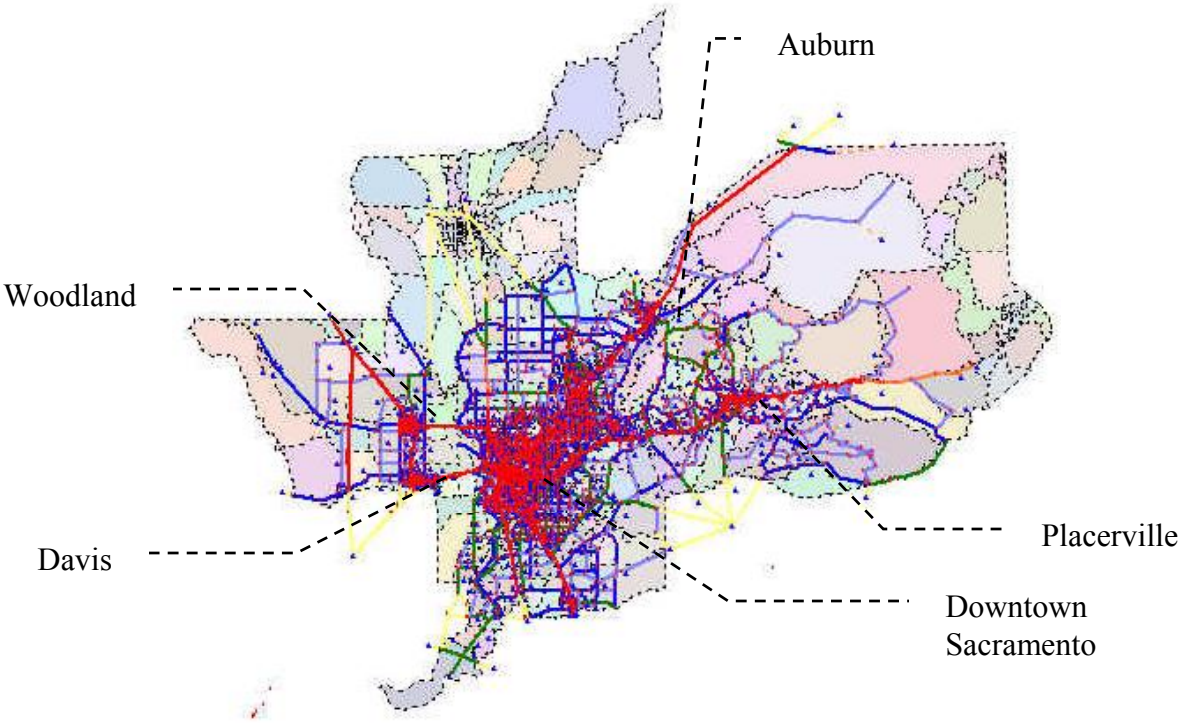

Figure 2. Grid Mesh Construction

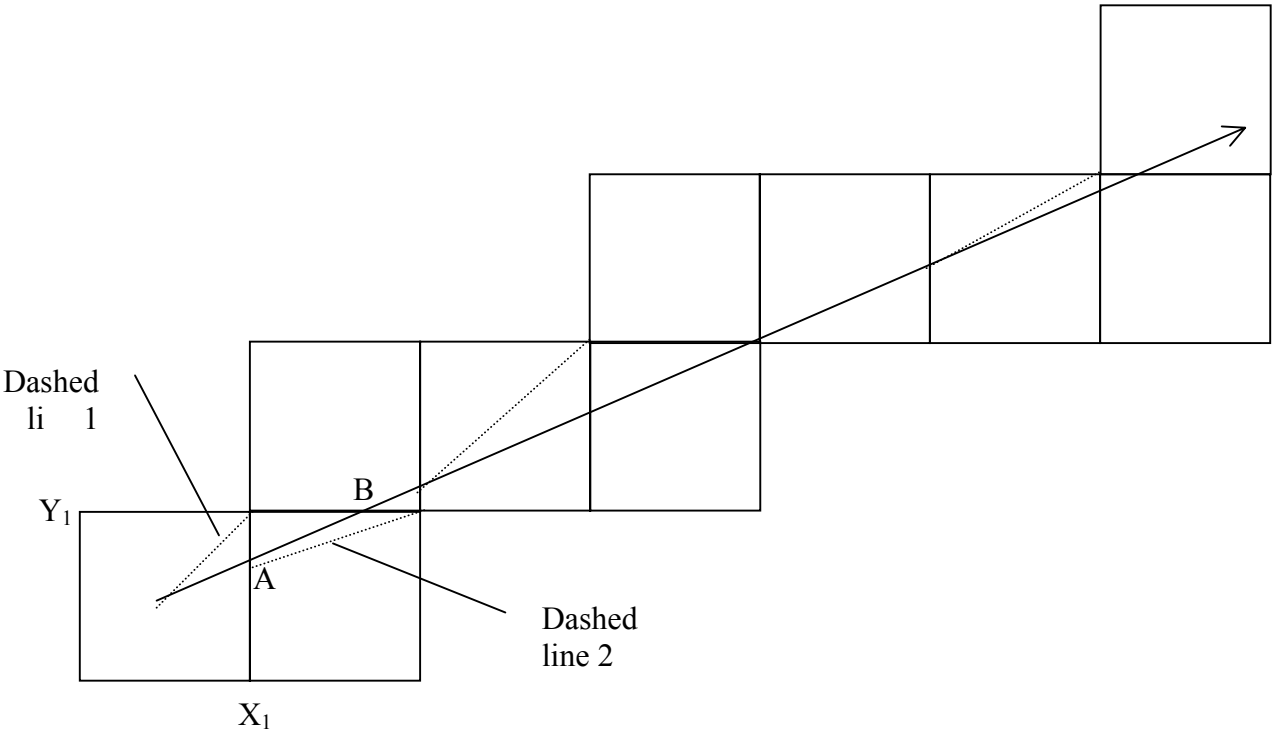

Figure 3. Intrazonal AM-Peak Activity Density at TAZ Centroids

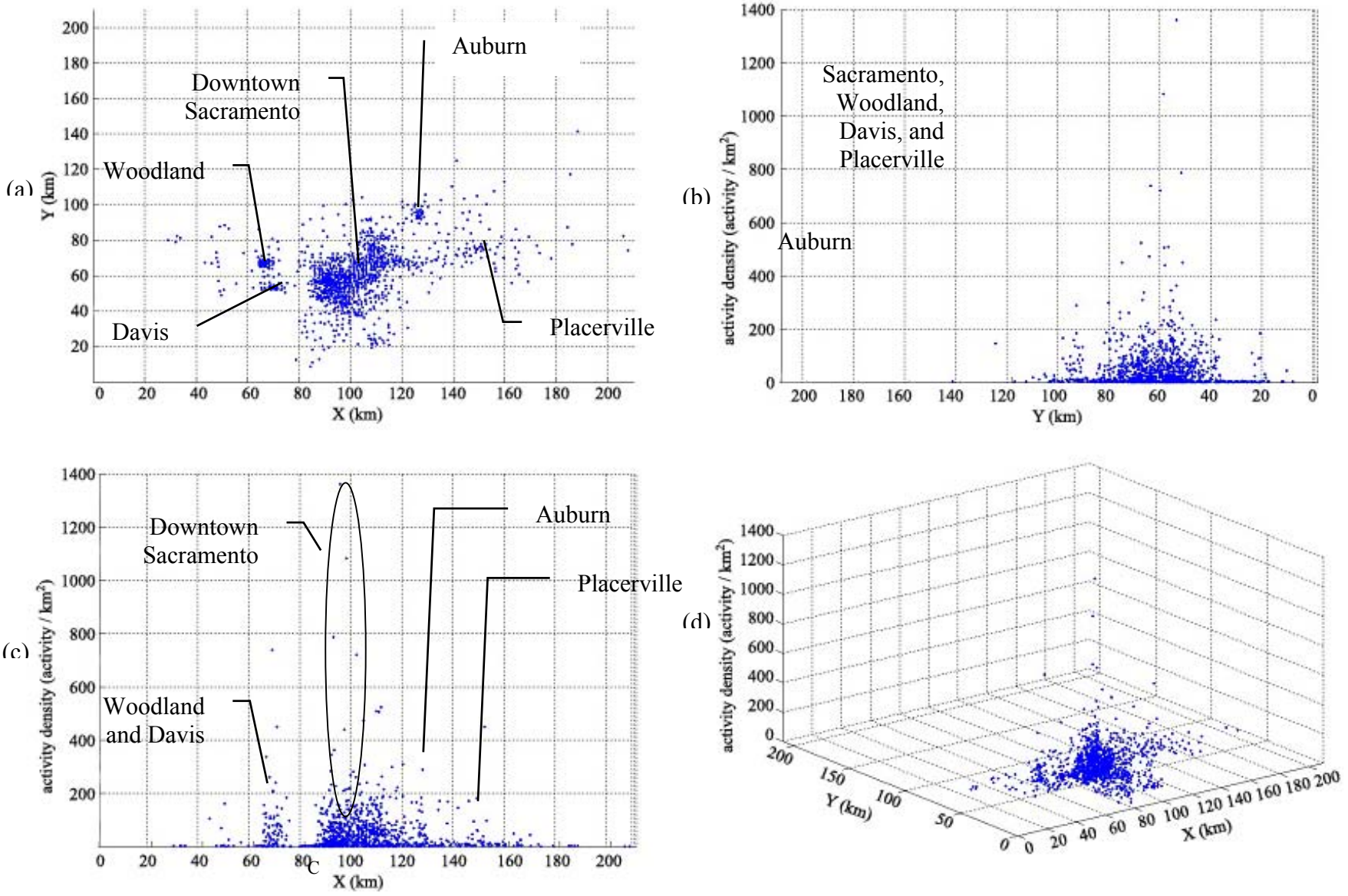

Figure 4. Interpolated Intrazonal AM-Peak Trip Density for Each Grid Cell

(a) Interpolated Activity Densities

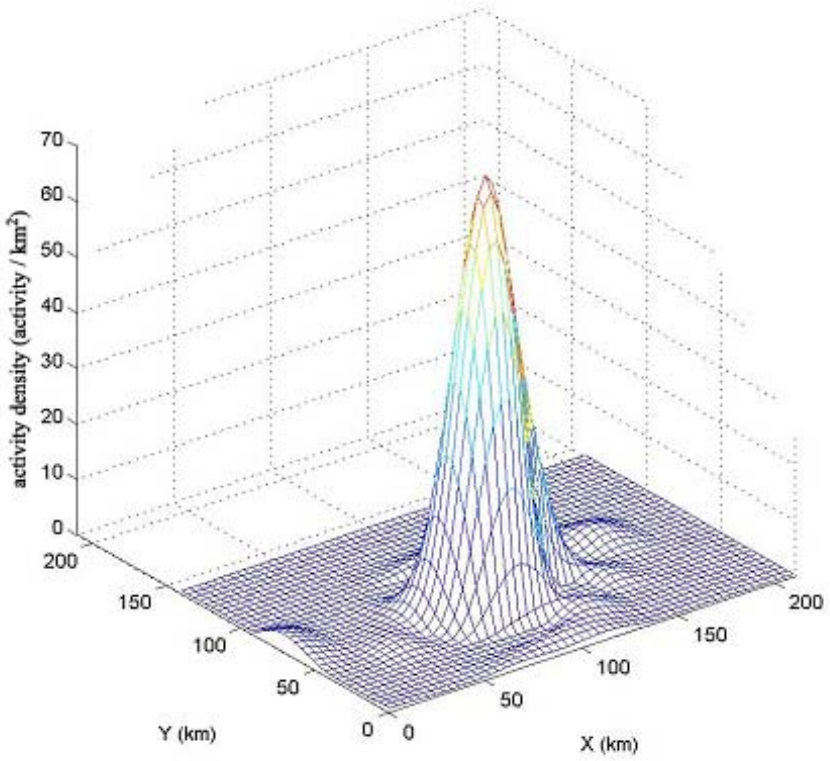

(b) Activity Densities (interval: 0.8 activities/km^2)

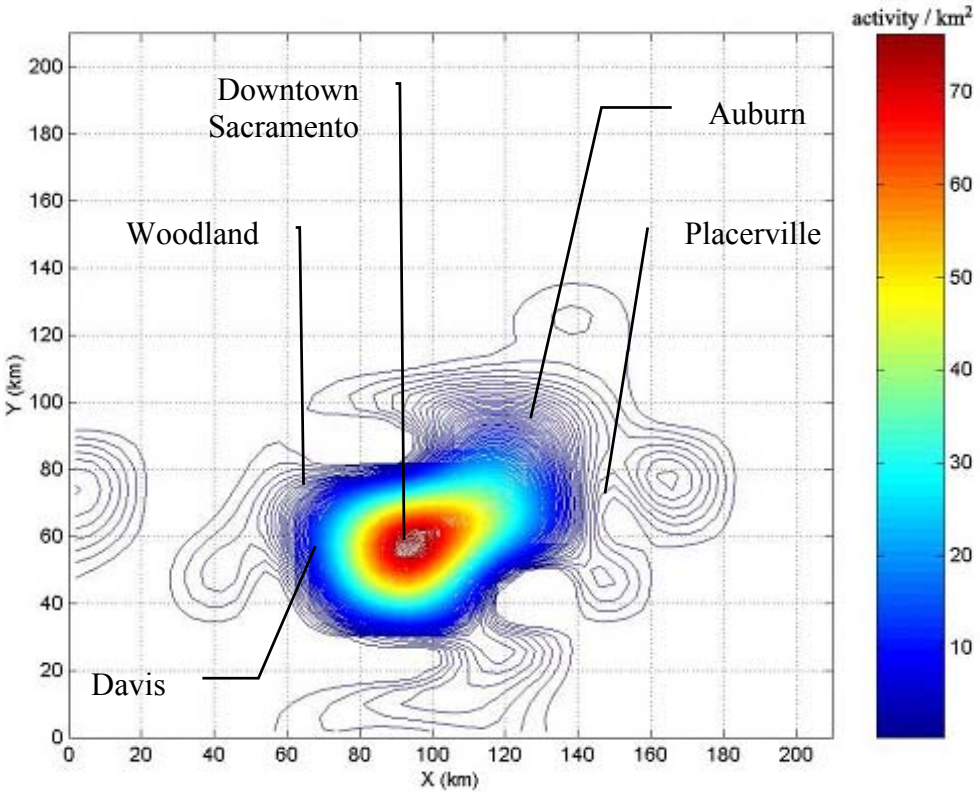

Figure 6. Gridded Intrazonal AM-Peak Emissions Using Proposed Allocation Factors

(a) Regional Spatial Allocation

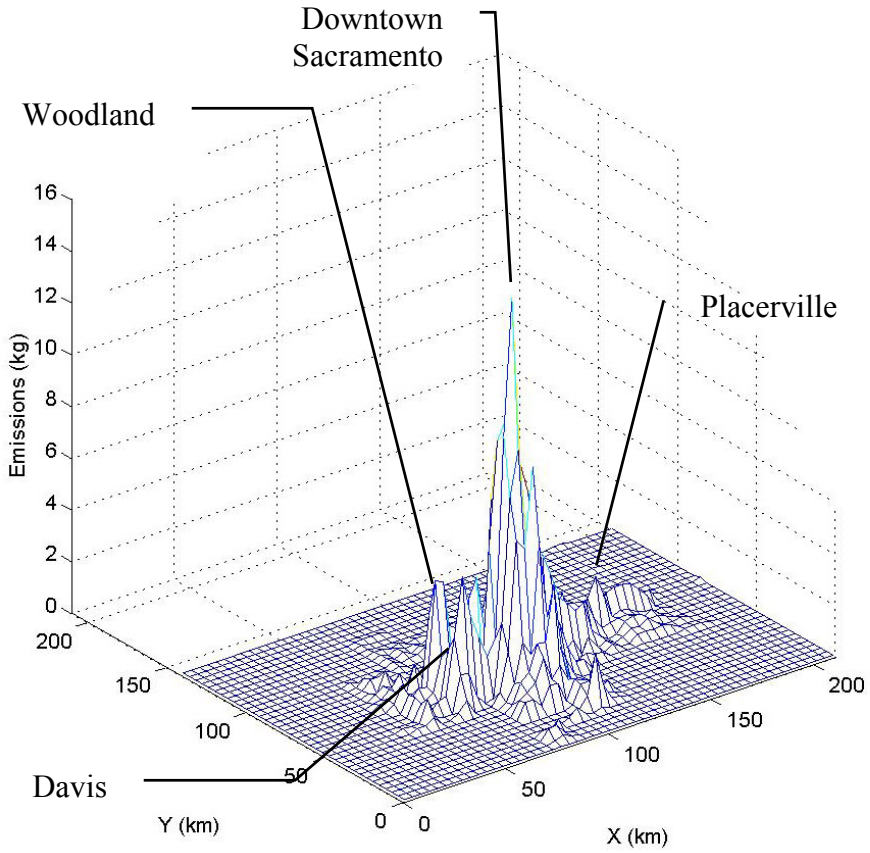

(b) Contour Plot (500 contour lines)

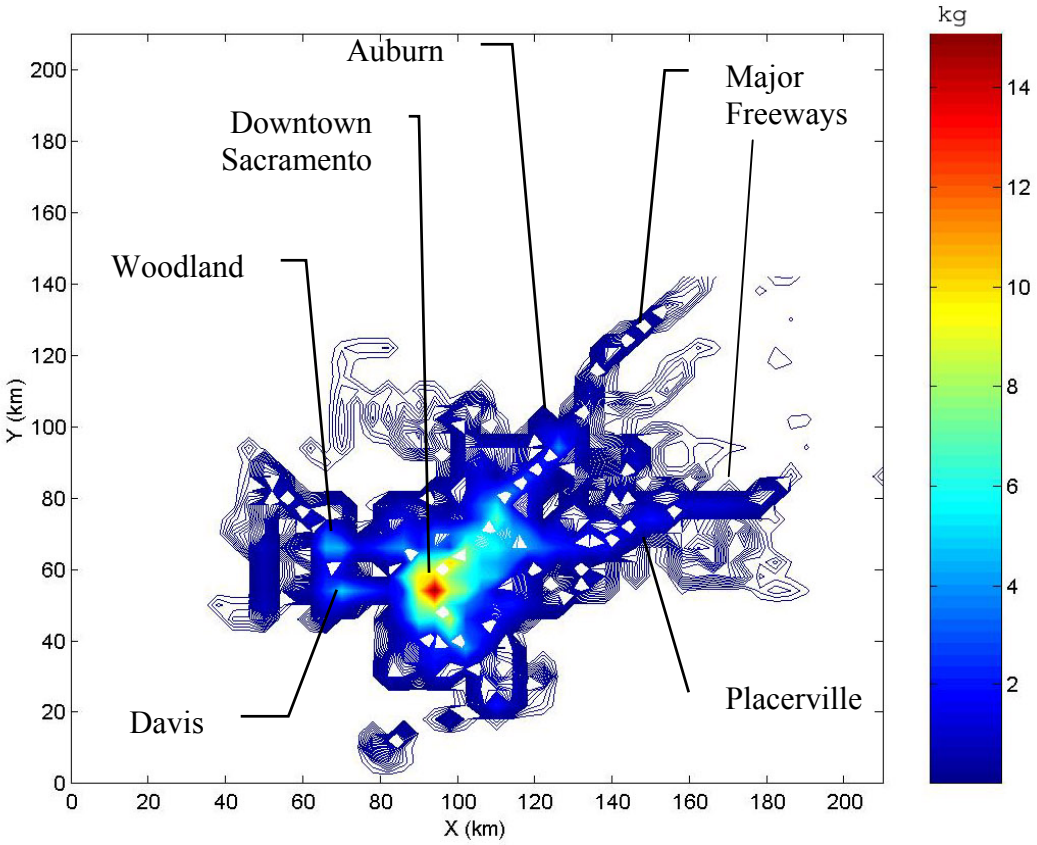

Figure 6. Gridded Intrazonal AM-Peak Emissions Using the Standard Gridding Protocol

(a) Regional Spatial Allocation

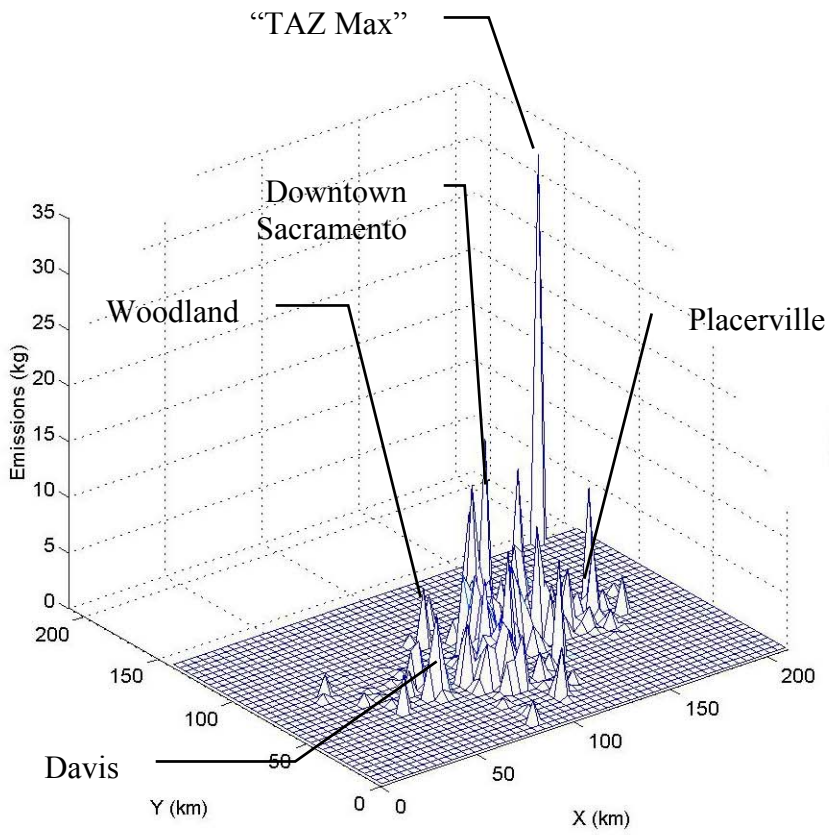

(b) Contour Plot (500 contour lines)

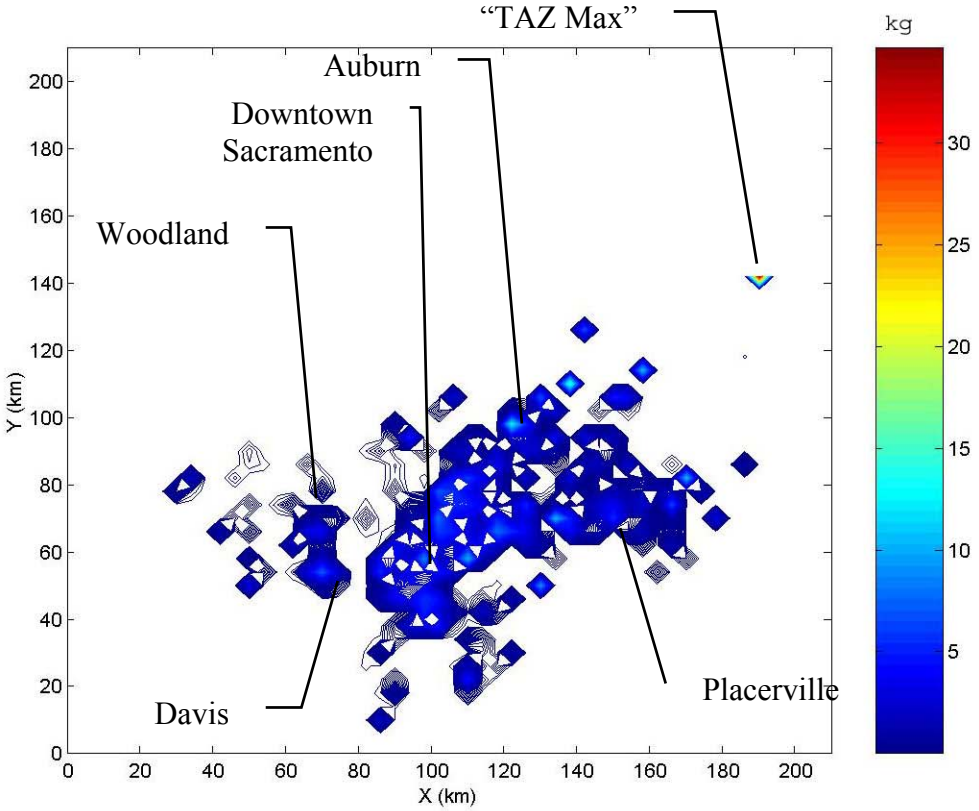

Figure 7. Interzonal Trip-End AM-Peak Activity Density at TAZ Centroids

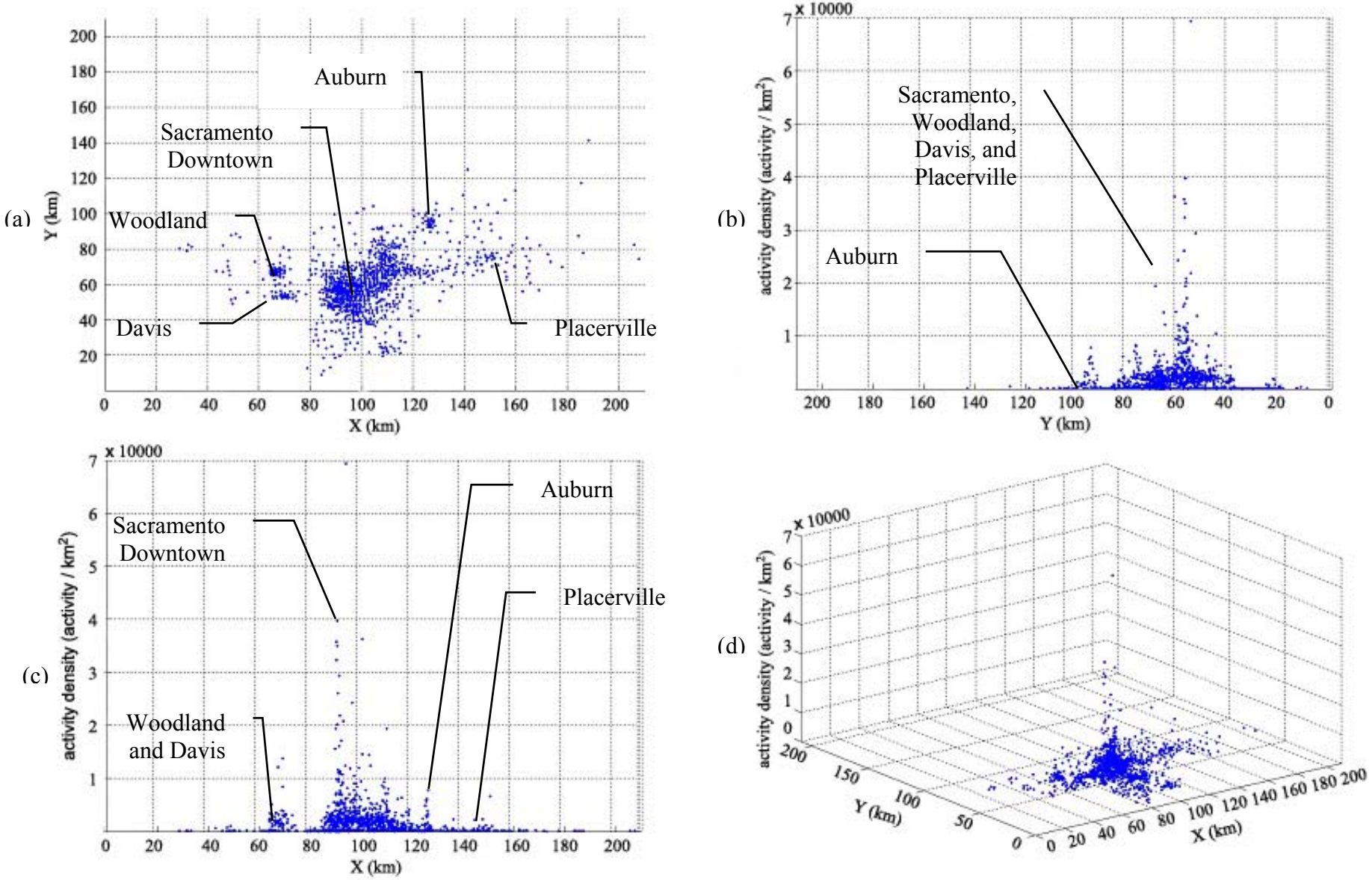

Figure 8. Interpolated Interzonal Trip-End AM-Peak Activity Density for Each Grid Cell

(a) Regional Spatial Allocation

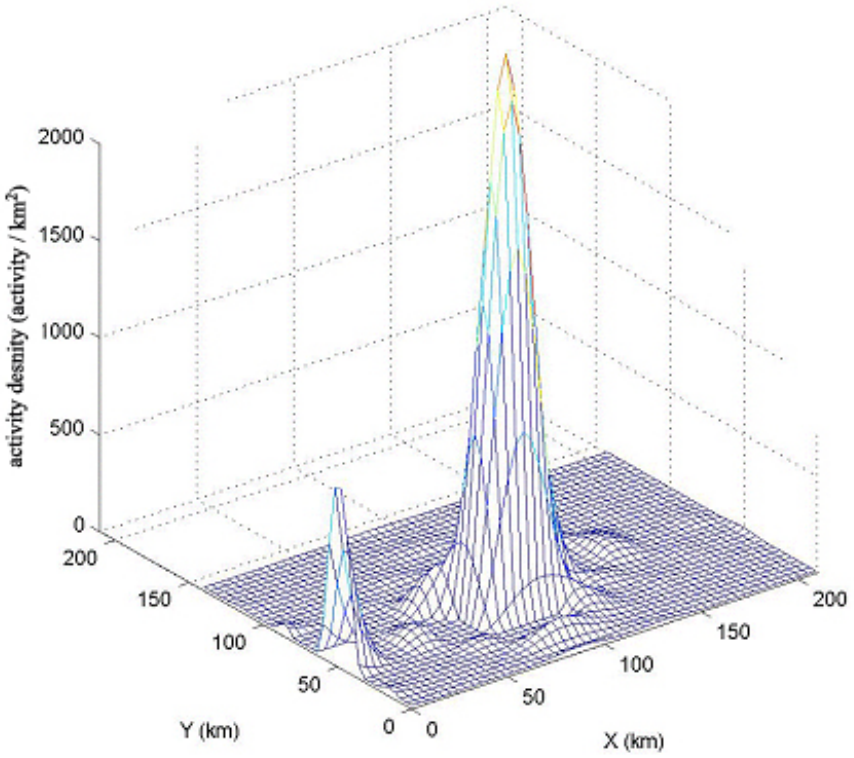

(b) Contour Plot (500 contour lines)

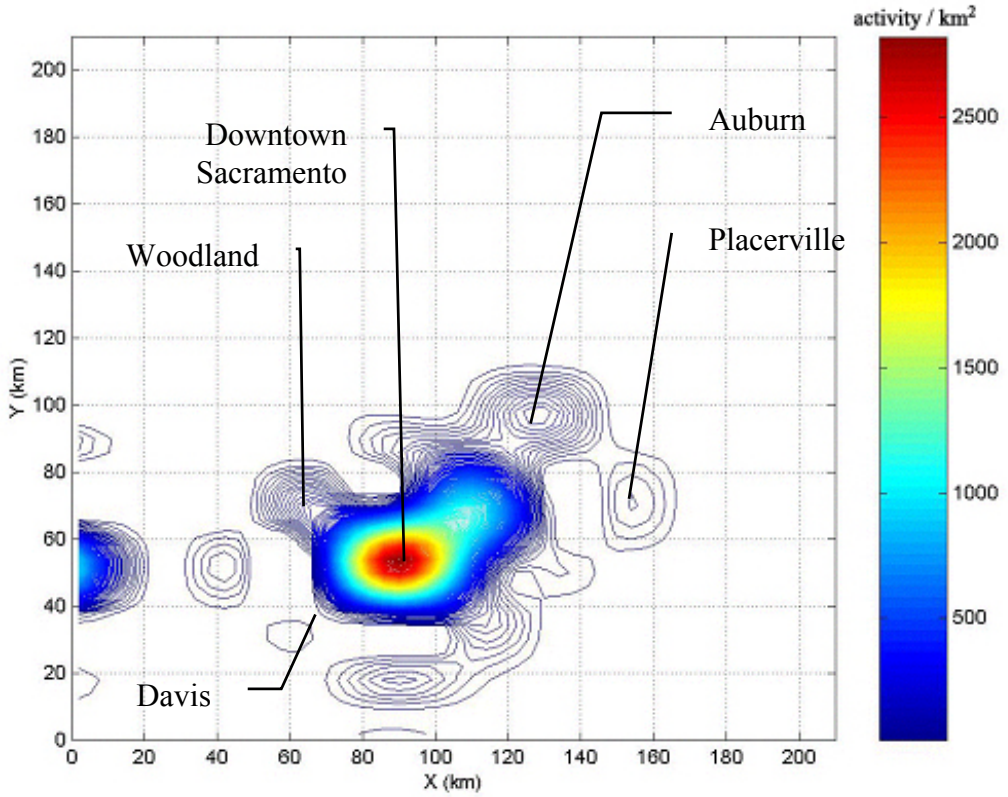

Figure 9. Gridded Interzonal Trip-End AM-Peak Emissions Using Proposed Allocation Factors

(a) Regional Spatial Allocation

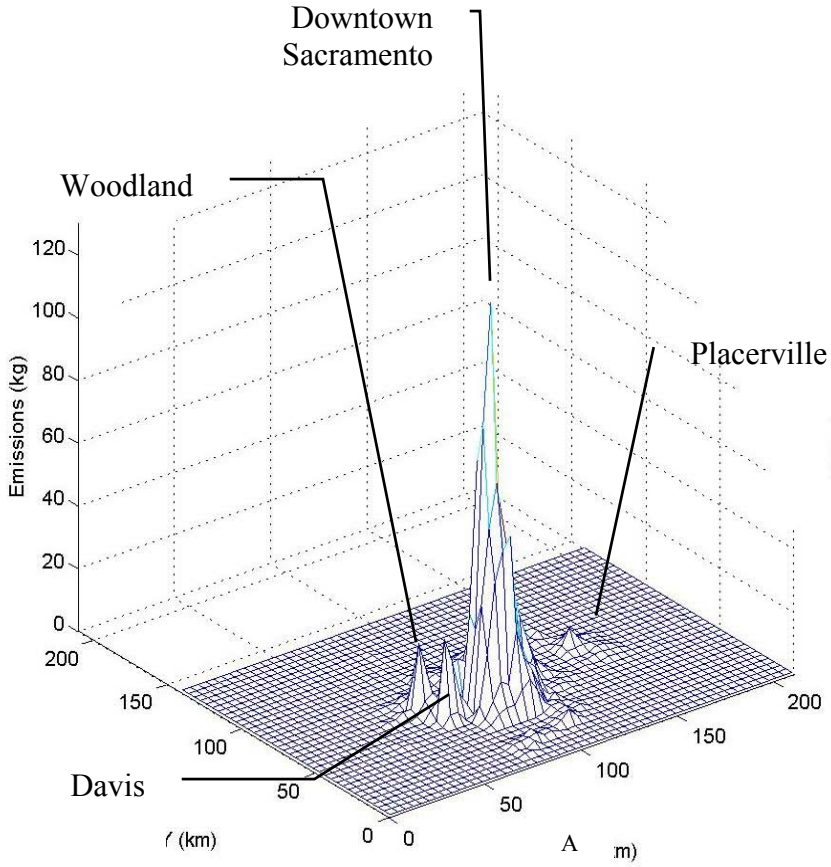

(b) Contour Plot (500 contour lines)

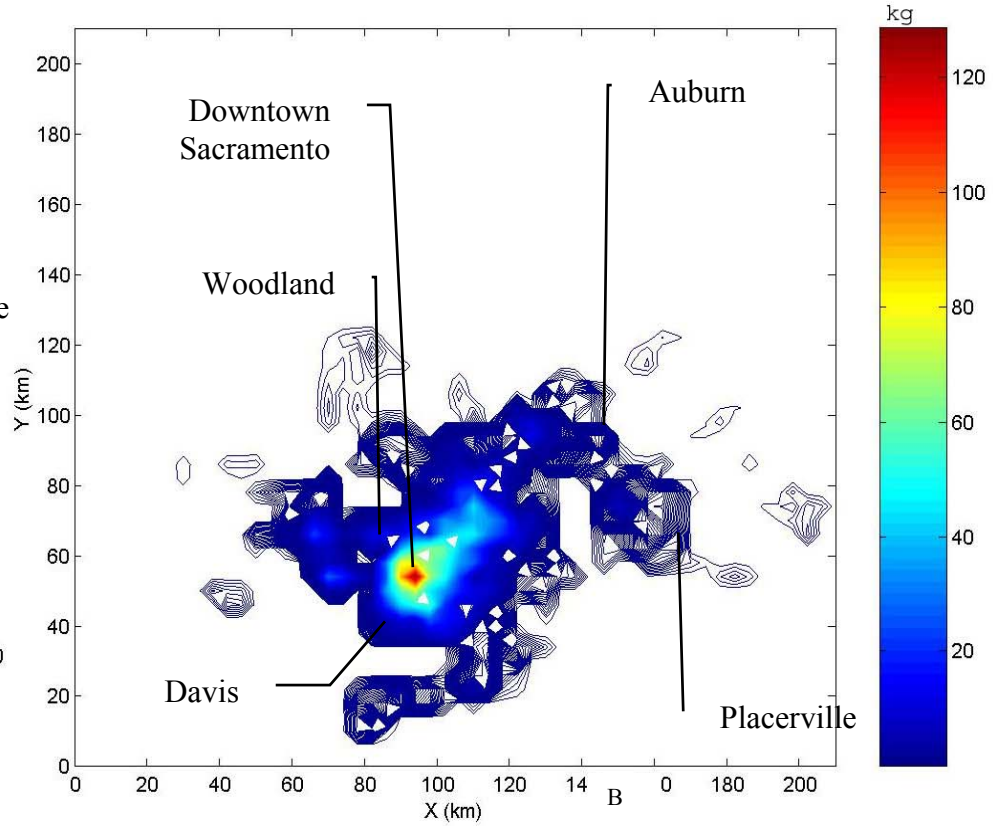

Figure 10. Interzonal Trip-End AM-Peak Emissions Using the Standard Gridding Protocol

(a) Regional Spatial Allocation

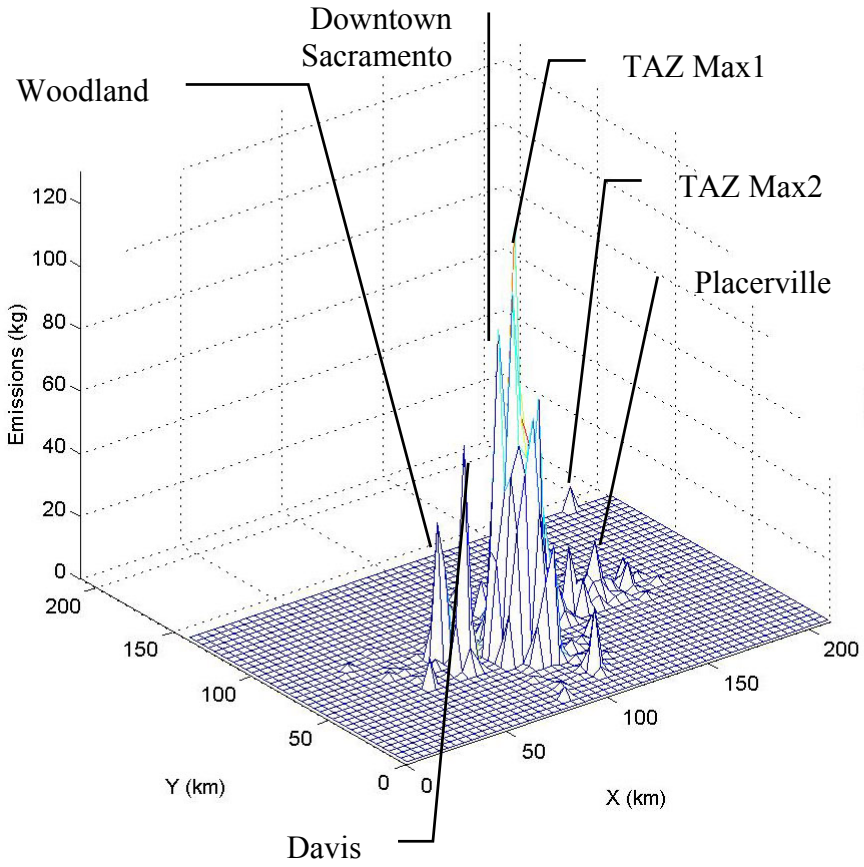

(b) Contour Plot (500 contour lines)